

Learning Driving Policies for End-to-End Autonomous Driving

Shoaib Azam, *Member, IEEE*, Farzeen Munir, *Member, IEEE*, and Moongu Jeon, *Senior Member, IEEE*,

Abstract—Humans tend to drive vehicles efficiently by relying on contextual and spatial information through the sensory organs.

Inspired by this, most of the research is focused on how to learn robust and efficient driving policies. These works are mostly categorized as making modular or end-to-end systems for learning driving policies. However, the former approach has limitations due to the manual supervision of specific modules that hinder the scalability of these systems. In this work, we focus on the latter approach to formalize a framework for learning driving policies for end-to-end autonomous driving. In order to take inspiration from human driving, we have proposed a framework that incorporates three RGB cameras (left, right, and center) to mimic the human field of view and top-down semantic information for contextual representation in predicting the driving policies for autonomous driving. The sensor information is fused and encoded by the self-attention mechanism and followed by the auto-regressive waypoint prediction module. The proposed method's efficacy is experimentally evaluated using the CARLA simulator and outperforms the state-of-the-art methods by achieving the highest driving score at the evaluation time.

Index Terms—Autonomous driving, Imitation learning, Attention, Driving Policies, Transformer.

1 INTRODUCTION

The automotive industry and autonomous vehicle startups are under pressure to generate revenues from billions of investments made in research and development over the past decade. But unfortunately, even though the experimental autonomous vehicle has continued their operation in limited cities, they continue to run into incidents, like autonomous vehicles blocking a fire truck while responding to an emergency. The autonomous vehicle faces dynamic and large-scale obstacles on the road, and counting each scenario into decision-making software is inconceivable, which hinders practical and scaleable deployment. The rare unfavorable events of long-tail distributions make it challenging to deploy modular design software for an autonomous vehicle compared to an end-to-end system for policy generation. The modular design consists of modules consisting of localization, perception, planning, and control. Each module provides coherent information to the next module for processing. The final input is then passed to the vehicle actuator for lateral and longitudinal control. This strategy is counterproductive and costly as each module is optimized for the input received from the previous module, and parameters are adjusted manually, which is very tedious and prone to error.

However, end-to-end learning techniques of the deep neural network provide a comprehensive approach for learning control policy for dynamic and unexpected traffic behaviors. These end-to-end approaches learn a mapping function that translates the input information of the dynamic environment using sensors such as cameras to control commands. Understanding the global context of the scene is an essential part of these end-to-end techniques, and in most of the previous research, a single camera modality is used

to determine the mapping function, which lacks sufficient knowledge for perceiving the driving scenes. In literature, researchers have fused data from Lidar and cameras to capture the 3D perspective of the surrounding environment. However, Lidar provides a sparse 3D representation of the environment, but dependence on Lidar data for practical and scaleable deployment for autonomous vehicles is an expensive solution.

This paper demonstrates the feasibility of generating driving policies by employing multiple cameras to obtain multi-perspectives and top-down 2D semantic map information to comprehensively understand the surrounding environment. To achieve this, we develop a framework that extracts features from input data and then fuses the features obtained and inputs them to a transformer network that forms the long-term relationship between the input features and output control commands. The learned features from the transformer are used to predict the waypoints for the autonomous vehicle to follow. We adopted the CARLA simulator to demonstrate the efficacy of the proposed framework. The main contributions of this work are:

- 1) Inspired by human driving, we proposed a framework to learn the driving policies for end-to-end autonomous driving. The proposed method utilizes the global contextual representation from the semantic information and spatial information from three RGB cameras in learning the driving policies.
- 2) The transformer encoder is used for learning the long-range dependencies between the embedded features. In addition, we encode the features from sensor modalities with velocity information to be utilized by the transformer encoder.
- 3) The evaluation of the proposed method is carried out using the CARLA simulator, and a comparative study illustrates that the proposed method outper-

Shoaib Azam, Farzeen Munir, and Moongu Jeon are with the School of Electrical Engineering and Computer Science, Gwangju Institute of Science and Technology, Gwangju, South Korea. e-mail: (shoibazam@gm.gist.ac.kr; farzeen.munir@gist.ac.kr; mgjeon@gist.ac.kr)

forms the baseline methods in terms of driving score and route completion, completing different traffic tasks.

The rest of the paper is organized as follows: Section 2 explains the literature review. Section 3 presents the proposed method framework and Section 4 corresponds to experimentation and results. Finally, Section 5 concludes the paper with possible directions of future work.

2 RELATED WORK

2.1 End-to-End Autonomous driving

End-to-end learning for realizing the control policies for autonomous vehicles using visual information is an active area of research [1]. Compared to the modular software stack for autonomous vehicles, end-to-end learning implicitly predicts waypoints or directly vehicular control commands using imitation learning [2]. The earlier work used only image data to determine the control policies, but recent research is focused on using multi-modal data. Multi-modal data leads to better scene understanding and allows learning multiple data representations. [3] proposed a model that uses RGB images and depth map to capture improved scene understanding and generalization of different driving scenarios. The fusion of features is demonstrated at low-dimensional latent features to generate a set of actions for the vehicle to follow. [4] explored segmentation-based visual abstraction to learn robust driving policies. Similarly, [5] conducted controlled experiments to learn explicit intermediate representation, which improved controlled driving policies. [6] focus on RGB images and Lidar data to have a global understanding of the surrounding. They proposed a multi-modal fusion transformer that integrates information at multiple stages to generate driving policies. [7] explored different stages of fusion of RGB and Lidar data and concluded that late-fusion was the best design. Each input modality is encoded as a separate branch and concatenated together. [8] employ dynamic vision camera and RGB camera and fuse the information using self-attention to train the network using imitation learning and determine the control policies.

Furthermore, Conditional imitation learning extends the imitation learning framework by integrating higher-level navigational directions into the decision-making process [9], but it is sensitive to new environments and weather conditions. A significant performance drop is observed when conditions are changed. The researcher employed simulators such as CARLA to simulate different environmental conditions and test the trained framework. [10] proposed a policy to map visual inputs to driving controls conditional to surrounding semantics and object affordance. Moreover, researchers have developed Reinforcement Learning (RL) agents to interact with simulated environments. [11] trained an RL expert agent that outputs low-level actions for autonomous vehicles using birds' eye view images. [12] proposed an interpretable RL framework that models complex urban scenarios in sequential latent representation and is jointly learned with behaviors policy for autonomous vehicles.

2.2 Transformer in End-to-End Autonomous driving

The transformer was initially developed for natural language processing tasks [13], but recently they have outperform classical neural networks in vision applications [14], [15]. The self-attention module in the transformer demonstrate improved global learning of sequential data and better feature representation. The researcher uses the transformer encoder to fuse multi-modal data. Transfuser exploits transformer block to combine intermediate features representation from RGB images, and Lidar data [6]. [16] proposed fusion Transformer, which inputs data from different view-point cameras and Lidar to learn the global context for comprehensive scene understanding and event detection. An encoder-decoder transformer configuration is employed to generate low-level actions for the ego vehicle's future trajectory. [17] design a transformer-based neural prediction framework that considers social interactions between different agents and generates possible trajectories for autonomous vehicles. [18] determine the driving direction from visual features acquired from images by using a novel framework consisting of a visual transformer. The driving directions are decoded for human interpretability to provide insight into learned features of the framework. [19], which considers social interaction between agents on the road and forecasts their future motion. The spatial-temporal dependencies were captured using a recurrent neural network combined with a transformer encoder.

3 METHOD

This section explains the proposed method for end-to-end learning control policies for autonomous driving. The proposed method is composed of two modules i) perception module and ii) waypoint prediction network. The following sections detail the problem formulation, input/output representation and model architecture, explaining the perception and waypoint prediction modules.

3.1 Problem Formulation

In this work, an end-to-end imitation learning approach is adopted for the point-to-point navigation problem, where the objective of the trained agent is to safely reach the goal point by learning a policy π^* that imitates the expert policy π . The learned policy completes the given route by avoiding obstacles and complying with the traffic rules. The expert policies are collected using the behavior cloning approach, a supervised learning approach of imitation learning, in a simulated environment. Suppose, the dataset $D = (X^j, Y^j)_{j=1}^d$ of size d is collected that consist of high dimensional observations X from the simulated sensory modalities along with the corresponding expert trajectories Y . The expert trajectories are defined in vehicle local coordinate space and are set of 2D waypoints transformed in bird's eye view (BEV) space, that is, $Y = y_t = (u_t, v_t)_{t=1}^T$, where u_t and v_t are the position information in horizontal and vertical directions, respectively. The objective is to learn the policy π with the collected dataset D in a supervised learning framework with the loss function \mathcal{L} as expressed in 1

$$\arg \min_{\pi} \mathbb{E}_{(X, Y) \rightarrow D} [\mathcal{L}(Y, \pi(X))]. \quad (1)$$

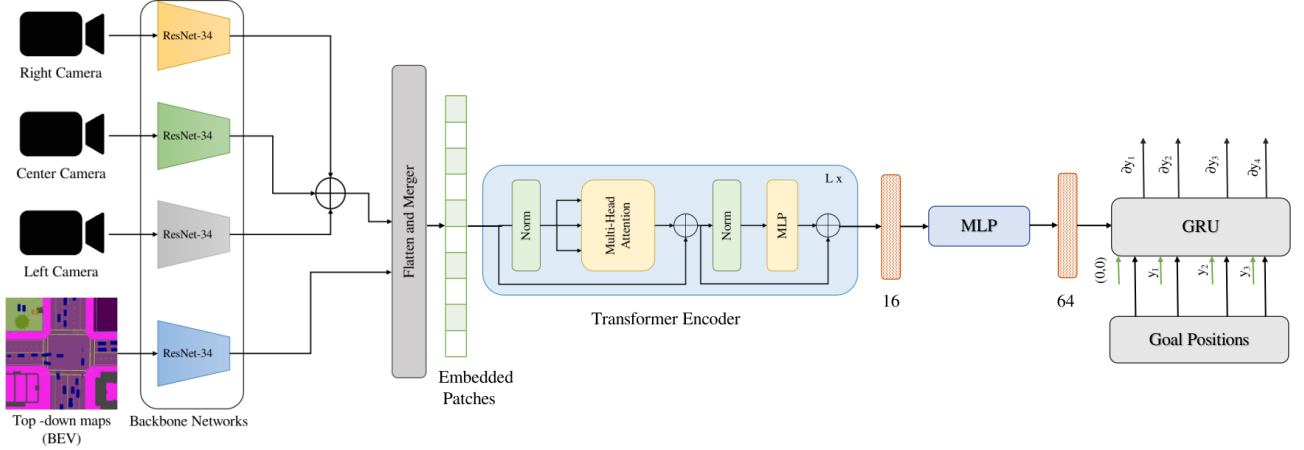


Fig. 1. The architecture of the proposed method which is comprised of two modules: perception block and waypoint prediction block. The perception module generates the features extracted from the input three RGB cameras (center, left, right) and the top-down semantic maps. These extracted features are then embedded with the velocity information to be utilized by the transformer encoder. The encoded features are then passed to the GRU-based waypoint prediction module for the generation of next waypoints. (Best view in color)

In this urban setting, the high-dimensional observations include the center, right and left camera and top-down semantic data for a single time step. It is to be noted here that in our problem setting, the single time step is used explicitly as prior work on using imitation learning for learning the control policies illustrate that observational histories have minimal effect on the performance gain.

3.2 Input and Output Representation

3.2.1 Input Representation

The proposed method utilizes two modalities: RGB cameras (left, center and right) and semantic maps. The three RGB cameras provide a complete field of view that mimics the human field of view. The semantic maps are converted to bird-eye view representation that contains ground-truth lane information, location, and status of traffic lights, vehicles, and pedestrians in the vicinity of ego-vehicle. The top-down semantic maps are cropped to the resolution of 256×256 pixels. For all three cameras, to cater the radial distortion, the resolution is cropped to 256×256 from the original camera's resolution of 400×300 pixels at the time of extracting the data.

3.2.2 Output Representation

For the point-to-point navigation task, the proposed method predicts the future trajectory Y of the ego-vehicle in the vehicle coordinate space. The future trajectory Y is represented by a sequence of 2D waypoints, $Y = y_t = (u_t, v_t)_{t=1}^T$, where u_t and v_t are the position information in horizontal and vertical directions, respectively. In the experimental analysis, we have utilized $T = 4$ as the number of waypoints.

3.3 Model Architecture

3.3.1 Perception Module

The perception module of the proposed method includes the backbone architecture and transformer encoder network. The following subsections explain the details of the perception module.

Backbone: For each input RGB image $I_{c,r,l} \in \mathbb{R}^{3 \times H \times W}$ from the center (c), right (r), and left (l) camera sensor, respectively, employ ResNet backbone for the feature extraction. Similarly, the top-down semantic representations from the semantic camera are color-coded first and then injected into the ResNet backbone for feature extraction. In this setting, the pre-trained ResNet model trained on the ImageNet dataset is utilized for generating the low-resolution feature maps $f \in \mathbb{R}^{C \times H \times W}$ for each sensor modality. The last layer of the ResNet model for each sensor modality generates $(B, 512, 8, 8)$ dimension feature maps, where B corresponds to batch size. The resolution of these resulting feature maps is reduced to the dimension of $(B, 512, 1, 1)$ by average pooling and flattened to a 512 dimension vector. In order to keep the features utilized by the transformer encoder, an additional projection layer is employed that transforms the resulting 512 dimension vector to a 400 dimension vector. Finally, all the 400 dimension vectors from each sensor modality that includes center, right, left, camera, and top-down semantic maps are concatenated to give the final 1600 dimension vector, which is then reshaped to $(B, 1, 40, 40)$ to be utilized by the transformer encoder. The following expressions in (2) summarize the computation of features maps in the backbone network for each sensor modality and top-down semantic maps,

$$\begin{aligned}
 I_{c,r,l}^{3 \times H \times W} &\xrightarrow{\text{Covn, bn, relu}} f_{c,r,l}^{64 \times 128 \times 128}, \\
 f_{c,r,l}^{64 \times 128 \times 128} &\xrightarrow{\text{maxpool}} f_{c,r,l}^{64 \times 64 \times 64}, \\
 f_{c,r,l}^{64 \times 64 \times 64} &\xrightarrow{l_1} f_{c,r,l}^{64 \times 64 \times 64}, \\
 f_{c,r,l}^{64 \times 64 \times 64} &\xrightarrow{l_2} f_{c,r,l}^{128 \times 32 \times 32}, \\
 f_{c,r,l}^{128 \times 32 \times 32} &\xrightarrow{l_3} f_{c,r,l}^{256 \times 16 \times 16}, \\
 f_{c,r,l}^{256 \times 16 \times 16} &\xrightarrow{l_4} f_{c,r,l}^{512 \times 8 \times 8}, \\
 f_{c,r,l}^{512 \times 8 \times 8} &\xrightarrow{\text{avgpool}} f_{c,r,l}^{512 \times 1 \times 1}, \\
 f_{c,r,l}^{512 \times 1 \times 1} &\xrightarrow{\text{flatten}} f_{c,r,l}^{512}, \\
 f_{c,r,l}^{512} &\xrightarrow{\text{proj}} f_{c,r,l}^{400} \xrightarrow{\text{reshape}} f_{c,r,l}^{1,40,40},
 \end{aligned} \tag{2}$$

where $H, W = 256$ respectively for each sensor modality and top-down semantic maps. The expressions mentioned above only illustrate the computation of feature extraction for a single batch. In our experiments, we have used the batch size of 64 to train the proposed method.

Transformer Encoder: In this work, a transformer encoder, specifically a vision transformer, is employed to learn the contextual relationship between the features and to generalize it to learn better feature representation. In this context, the resulting features $f = \mathbb{R}^{1 \times H \times W}$ is fed to the transformer encoder by flattening into patches $f_p = \mathbb{R}^{N \times (P^2 C)}$, where H and W corresponds to the resolution of input features from the backbone network, C is the number of channels, (P, P) is the size of each patch, and $N = HW/P$ illustrates the number of patches and also the input sequence length. In addition, a learnable position embedding is added to the input sequence, a trainable parameter with the same dimension as the input sequence, so that the network infers the spatial dependencies between different tokens at the train time. A velocity embedding is also added to the C dimension of the input sequence through a linear layer, which includes the current velocity. Finally, the input sequence, positional embeddings E_{pos} , and velocity embeddings E_{vel} are element-wise summed together, which is mathematically expressed as following (3),

$$\begin{aligned} z_o &= [f_p^1 E; f_p^2 E; \dots; f_p^N E] + E_{pos} + E_{vel}, \\ E &\in \mathbb{R}^{(P^2 \cdot C) \times D}, \\ E_{pos} &\in \mathbb{R}^{(N+1) \times D}, E_{vel} \in \mathbb{R}^{(N+1) \times D}, \\ z'_l &= MSA(LN(z_{l-1})) + z_{l-1} + z_{l-1}, \\ z_l &= MLP(LN(z'_l)) + z'_l + z'_l, \end{aligned} \quad (3)$$

where MSA corresponds to multi-head self-attention, MLP is multi-layer perceptron, LN is layer normalization, and D corresponds to dimension. The mathematical formulation of the multi-head self-attention is shown in Eqs (4)

$$\begin{aligned} (\mathbf{Q}, \mathbf{K}, \mathbf{V}) &= \mathbf{z} \mathbf{W}_{QKV}, \\ \mathbf{W}_{QKV} &\in \mathbb{R}^{D \times 3D_h}, \\ A &= softmax(\mathbf{Q} \mathbf{K}^T) / \sqrt{D_h}, \\ A &\in \mathbb{R}^{N \times N}, \\ SA(\mathbf{z}) &= \mathbf{A} \mathbf{v}, \\ MSA(\mathbf{z}) &= [SA_1(\mathbf{z}); SA_2(\mathbf{z}); \dots; SA_j(\mathbf{z})] \mathbf{W}_{msa}, \\ \mathbf{W}_{msa} &\in \mathbb{R}^{(j \cdot D_h) \times D}. \end{aligned} \quad (4)$$

where Q, V and K are the query, value and key vectors and W is the weight matrix. The output features from the MSA have the same dimension as the input features. The transformer encoder applies the attention multiple times throughout the architecture. The final output features from the transformer encoder are then summed along the dimension to produce the 16 dimensional vector having the contextual representation of features from all the sensor modalities. This resulting 16 dimensional feature vector is injected into the waypoint prediction module to predict waypoints.

3.3.2 Waypoint Prediction Module

The waypoint prediction module acts as a decoder for predicting the waypoints using the encoded information

from the transformer encoder. The resulting 16 dimensional vector is passed through an MLP consisting of two hidden layers having 256 and 128 units, respectively, to output the 64 dimension vector. The MLP layer is used for upsampling the vector dimension from 16 to 64 and is related to experimental heuristics that produce better results in terms of waypoint prediction. We have employed the auto-regressive GRU model to predict the next waypoints that take the 64 dimension feature vector to initiate the hidden state of the GRU model. The GRU-based auto-regressive model takes the current position and goal location as input, which helps the network focus on the relevant context in the hidden states to predict the next waypoints. The goal locations include the GPS points registered in the same ego-vehicle coordinate frame as input to the GRU rather than the encoder because of the colinear BEV space between the predicted waypoints and the goal locations. In order to predict the next waypoints, a single layer GRU layer followed by a linear layer is employed to predict $T = 4$ future waypoints in the ego-vehicle coordinate frame. Initially, the first unit of GRU is inputted by $(0, 0)$ since the BEV space is centered with the ego vehicle's position.

The predicted waypoints are then passed to the control module to generate steer, throttle, and brake values. In this context, two PID controllers for lateral and longitudinal control are used. The longitudinal controller takes the average weighted magnitude of vectors between the waypoints of consecutive time steps, whereas the lateral control takes their orientation. For the control settings, we have used the settings as suggested by the following codebase benchmarked on the CARLA dataset.

3.4 Experiments and Results

This section explains the experimental setup for dataset collection, evaluation metrics, training details, and experimental results of the proposed method compared to the state-of-the-art methods.

3.4.1 Dataset

In this work, we have utilized CARLA 0.9.10 simulator to generate the dataset. The CARLA simulator provides 8 publically available town. In our experimentation, we have used 7 towns to generate the training dataset, and Town05 is used to evaluate the proposed method due to the large diversity in traffic scenarios; for instance, single and multi lanes roads, highways, bridges, and underpasses. Table 1 illustrates the dataset details that are utilized in generating the training dataset to create a more varying simulation environment. In addition, the non-player-characters (NPC) are also spawned in the simulation to mimic real-world conditions. For generating the dataset, an expert policy with the privileged information from the simulation is rolled out to save the data at 2FPS. The dataset includes left, right, and center camera RGB images, top-down semantic map information, the corresponding expert trajectory, speed data, and vehicular controls. The trajectory includes 2D waypoints transformed into bird-eye-view (BEV) space in the vehicle's local coordinate, whereas the steering, throttle, and brake data are incorporated into the vehicular control data at the time of recording. Inspired by [6] configurations,

TABLE 1
Dataset generation details using the CARLA simulator for the proposed method

Maps	Training Data: Town01, Town02, Town03, Town04, Town06, Town07, Town10 Test Data: Town05
Weather Conditions	Clear sunset, Clear noon, Wet noon, Wet sunset, Cloudy noon, Cloudy sunset, Rainy noon, Rainy sunset
Non-player characters (NPCs)	Pedestrians, Car, Bicycle, Truck, Motorbike
Object Classes	0:Unlabeled, 1:Pedestrian, 2:Road line, 3:Road, 4:Sidewalk, 5:Car, 6:Red traffic light, 7: Yellow traffic light, 8: Green traffic light
Routes	Tiny (only straight or one turn) Short (100-500m) Long (1000-2000m)
CARLA Version	0.9.10

we have gathered the data by giving a set of predefined routes to the expert in driving the ego-vehicle. The GPS coordinates define the routes provided by the global planner and high-level navigational commands (e.g., turn right, follow the lane, etc.) The routes are categorized into three settings: long, short, and tiny. In the long routes settings, the expert must drive 1000 – 2000 meters, including 10 intersections for each. On the short routes set, the expert must drive 100 – 500 meters having 3 intersections for each. The tiny routes set include only one driving configuration, for instance, one turn or one straight go, that the expert must complete during the simulation. We have generated around 60 hours of the dataset, including 200K frames.

3.4.2 Evaluation Metrics

The proposed method's efficacy is evaluated using the following metrics indicated by the CARLA.

(1) **Route Completion (RC):** is the percentage of route distance R_j completed by the agent in route j averaged across the number of N routes is shown in Eq.(5),

$$RC = \frac{1}{N} \sum_j^N R_j. \quad (5)$$

The RC is reduced if the agent drives off the specified route by some percentage of the route. This reduction in RC is defined by a multiplier (1-% off route distance).

(2) **Infraction Multiplier (IM):** as shown in Eq.(6) is defined as the geometric series of infraction penalty coefficient, p^i , for every infraction encountered by the agent along the route. Initially, the agent starts with the ideal base score of 1.0, which is reduced by a penalty coefficient for every infraction. The penalty coefficient p^i for each infraction is predefined. If the agent collides with the pedestrian $p_{pedestrian}$, the penalty is set to 0.50; with other vehicles $p_{vehicles}$, it is set to 0.60, 0.65 for collision with static layout p_{stat} , and 0.7 if the agent breaks the red light p_{red} . The penalty coefficient is defined as $PC = p_{pedestrian}, p_{vehicles}, p_{stat}, p_{red}$,

$$IM = \prod_i^{PC} (p^i)^{infractions^i}. \quad (6)$$

(3) **Driving Score (DS):** is computed by taking the product between the percentage of the route completed by the agent R_j and the infraction multiplier IM_j of the route j and averaged by the number of the routes N_r . The

higher the driving score corresponds to the better model. Mathematically, the driving score (DS) is shown in Eq.(7),

$$DS = \frac{1}{N_r} \sum_{j=1}^{N_r} RC_j IM_j (p^i)^{infractions^i}. \quad (7)$$

It is to be noted that if the ego vehicle deviates from the route j for more than 30 meters or there is no action for 180 seconds, then the evaluation process on route j will be stopped to save the computations cost and next route will be selected for the evaluation process.

3.4.3 Training Details

The proposed method is trained using the dataset collected from the CARLA simulator by rolling out the expert model. In addition, we have used the pre-trained ResNet model trained on the ImageNet dataset to extract the features in the backbone network for each sensor modality. In training the proposed network, we have added augmentation such as rotating and noise injection to the training data, along with adjusting the waypoints labels. For the transformer encoder, we have used the patch size of 4, which gives the 16 dimensional feature embedding. We have trained the proposed method using the Pytorch library on RTX 3090 having 24 GB GPU memory for a total of 100 epochs. In training, we have used the batch size of 64 and an initial learning rate of 10^{-4} , which is reduced by a factor of 10 after every 20 epochs. The L_1 loss function is used for training the proposed method. Let y_t^{gt} represent the ground-truth waypoints from the expert for the timestep t ; then the loss function is represented by the Eq.(8),

$$\mathcal{L} = \sum_{t=1}^T \|y_t - y_t^{gt}\|_1. \quad (8)$$

An AdamW optimizer is used in training with a weight decay set to 0.01 and beta values to the Pytorch defaults of 0.9 and 0.99. For every 5 epoch, the model is evaluated on the validation routes, and the epoch which gives the highest driving score is saved.

3.4.4 Results

The proposed method's efficacy is evaluated in different traffic scenarios using Town05 of the CARLA simulator. For the quantitative comparison, we have considered the following baseline methods. (1) **CIRLS** [20] is the conditional imitation learning method in which the agents tend to learn the driving policies conditioned on a high-level navigational

TABLE 2

Quantitative comparison between the proposed method and the baseline state-of-the-art methods. The comparative analysis is based on better driving and route completion scores. The proposed method evaluation scores in terms of driving and route completion scores are better than the baseline state-of-the-art methods.

Model	Town05 Short		Town05 Long	
	Avg. Driving Score (DS) \uparrow	Avg. Route Completion (RC) \uparrow	Avg. Driving Score (DS) \uparrow	Avg. Route Completion (RC) \uparrow
CILRS [20]	7.47	13.40	3.68	7.19
LBC [21]	30.97	55.01	7.05	32.09
AIM [6]	49.00	81.07	26.50	60.66
Late Fusion [6]	51.56	83.66	31.30	68.05
Geometric Fusion [6]	54.32	86.91	25.30	69.17
Transfuser [6]	54.52	78.41	33.15	56.36
SDC [22]	58.357	84.270	40.21	52.43
Ours	63.127	87.565	48.78	57.67
Expert	84.67	98.59	38.60	77.47

command using only a single front camera as a sensor modality. (2) **LBC** [21] corresponds to the knowledge distillation approach in which, first, a teacher agent is trained having access to the ground-truth BEV semantic maps for the prediction of waypoints using the expert data. Later, an image-based student model with the teacher model's supervision is trained to learn the driving policies. It is to be noted that only image data is available to the student model at the time of training and cannot access privileged map information. We also explored the sensor fusion-based method for learning the driving policies in the experimental analysis. In this context, (3) the **Transfuser** [6] model is considered for the comparative analysis. In this method, Lidar and RGB camera data are fused at multiple levels using the self-attention transformer model, and then the policies are determined by using an autoregressive waypoint prediction model. This approach forms the baseline for the proposed method. Inspired by [6], we have re-implemented the other three models along with the Transfuser model for the comparative analysis. Moreover, these models include AIM, Geometric fusion, and the Late-fusion methods to analyze the effect of sensor fusion concerning the proposed method. (4) **AIM** [6] is an autoregressive image-based waypoint prediction model that uses only single camera input for the waypoint prediction. The latter two methods, geometric and late fusion, employ the fusion of RGB camera and Lidar for predicting the driving policies. (5) The **geometric fusion** [6] uses the multi-scale geometry based fusion as discussed in [23] [24]. It involves both paradigms of fusion from image-to-Lidar and Lidar-to-image feature fusion. (6) **The late fusion** [6] involves the feature fusion at the end after each encoder network extracts the RGB camera and Lidar features. This fusion is the element-wise summation of features, and then the fused feature is passed to the waypoint prediction network for learning the driving policies. Another baseline model SDC [22], uses the BEV semantic depth cloud for learning end-to-end driving policies. The input to the encoder network is from RGB images and depth information, GPS, and speedometer information. The encoded features are then passed to the controller block that includes the GRU for predicting the waypoints. It is to be noted that in our experimentation, we have replicated the baseline models to make a comparative analysis with the proposed method. In addition, since the training of the proposed method involves different environmental conditions,

we evaluated the proposed method with the other baselines only on ClearNoon weather conditions to better analyze the generalization of the proposed method.

The quantitative comparison is performed on the evaluation metrics of driving score (DS), route completion (RC), and the infraction multiplier (IM). The essential evaluation metric based on which the proposed method and the baseline methods are evaluated is the driving score (DS), which is the product of route completion (RC) and the infraction multiplier (IM). The higher the driving score corresponds to a better model evaluation. It is also to be noted that the model may have high RC and IM, but this does not satisfy that the model has performed better than the driving score (DS) evaluation metric. Table 2 illustrates the quantitative comparison between the proposed method and the baselines. The CILRS model has a low driving and route completion score compared to the proposed method. The reason for this is the improper balance between the navigational commands that result in the poor performance of the CILRS model. The LBC model performs significantly better than the CILRS model because of the supervision provided by the teacher network to the image-based student model, yet the driving score and the route completion illustrate that the LBC model fails to handle complex urban driving scenarios. The LBC and CILRS performance significantly drops when tested on the long routes of Town05. The AIM image-based model's evaluation improves the driving and route completion score compared to LBC and CILRS by adding the autoregressive waypoint method on the decoder side. However, the AIM model evaluation illustrates the improvement, yet compared to the proposed method, its performance in terms of driving score and route completion is not promising, leaving room for the fact that by fusing different sensor modalities data, the driving policies can be learned better. The comparative analysis between the sensor fusion method that includes late fusion, geometric fusion, Transfuser, and SDC has shown promising results in learning the driving policies in comparison to the CILRS, LBC, and AIM models but cannot perform better compared to the proposed method because of not providing the contextual representation of the environment by covering the whole field of view and semantic information. The intriguing question is that Lidar, in the form of point-cloud data, provides complete information about the environment but the problem with this data is the sparsity and limited spatial resolution. The

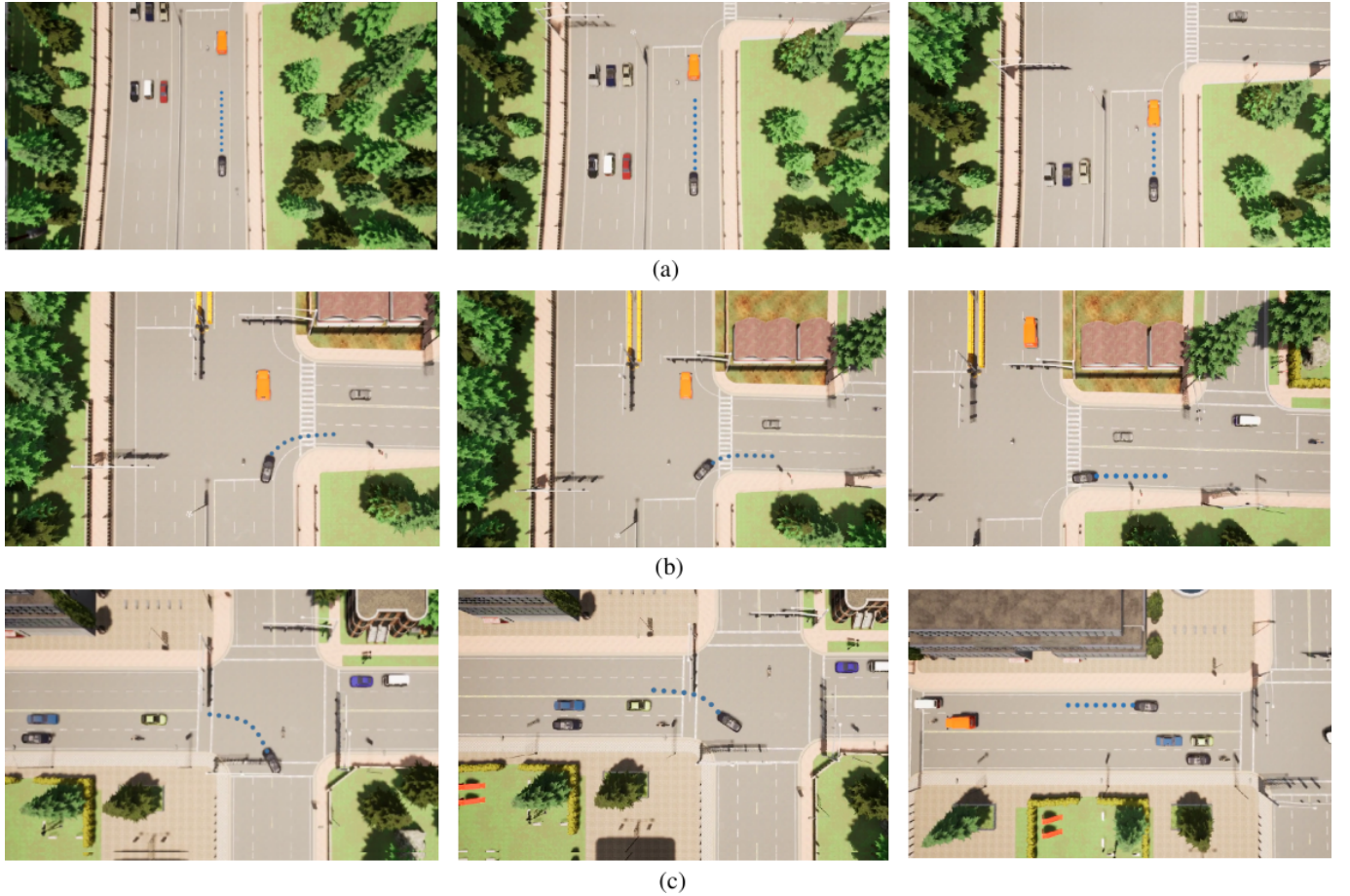


Fig. 2. Qualitative results for the proposed method in different driving conditions. In urban driving conditions, the proposed method is evaluated on Town05 dataset of CARLA simulator, illustrating the performance of learned driving policies using the proposed method on straight roads, keeping in the lane, and turning left and right respectively. (a) illustrates the driving policy is evaluated on the straight road while the ego-vehicle keeps in the lane. (b) shows the behavior of ego-vehicle by using the learned driving policy evaluated on the right turns. (c) Similarly, the learned driving policy using the proposed method is illustrated on the left turn.



Fig. 3. Qualitative results for the learned driving policies using the proposed method on stopping at red traffic light.

proposed method has performed better than the baseline methods and achieved a driving score of 63.127 and 87.565 in the route completion for short routes. Similarly, for the long routes, the proposed method has achieved a driving score of 48.78 and a route completion score of 57.67.

We illustrate the proposed method's efficacy in different tasks for qualitative analysis as shown in Fig.2 and Fig.3, respectively. The learned driving policy through the proposed method is displayed in moving straight, stopping at the traffic light, and making left, and right turns. These results illustrate that the policy learned using the proposed method show promising results and complements the quantitative analysis of the proposed method with other state-of-the-art

baseline methods.

4 CONCLUSION

In this work, we have proposed a framework for learning driving policies for end-to-end autonomous driving. The proposed method is composed of two modules: the perception module and the waypoint prediction module. In order to incorporate the spatial and contextual information about the environment, the perception module receives the data from three RGB cameras and top-down semantic information. First, the features are extracted through the backbone network in the perception module. Then, the resulting features are fused and embedded with velocity information. The embedded features are then passed to the transformer encoder to learn the long relation dependencies between the features. Finally, the GRU-based waypoint prediction network processes the encoded features to output the next waypoints. For the comparative analysis, the proposed method is quantitatively compared with the state-of-the-art methods, resulting in better driving and route completion scores. Further, to demonstrate the effectiveness of the proposed method, the qualitative results are presented in different driving situations, illustrating that

the driving policies learned using the proposed method perform better. The future work includes improving the perception module by adding the radar data, which complements the camera data. In addition, the proposed method can be utilized by designing a neural-network controller or a model predictive-based controller.

REFERENCES

- [1] J. Janai, F. Güney, A. Behl, A. Geiger *et al.*, "Computer vision for autonomous vehicles: Problems, datasets and state of the art," *Foundations and Trends® in Computer Graphics and Vision*, vol. 12, no. 1–3, pp. 1–308, 2020.
- [2] A. Tampuu, T. Matiisen, M. Semikin, D. Fishman, and N. Muhammad, "A survey of end-to-end driving: Architectures and training methods," *IEEE Transactions on Neural Networks and Learning Systems*, 2020.
- [3] Z. Huang, C. Lv, Y. Xing, and J. Wu, "Multi-modal sensor fusion-based deep neural network for end-to-end autonomous driving with scene understanding," *IEEE Sensors Journal*, vol. 21, no. 10, pp. 11 781–11 790, 2020.
- [4] A. Behl, K. Chitta, A. Prakash, E. Ohn-Bar, and A. Geiger, "Label efficient visual abstractions for autonomous driving," in *2020 IEEE/RSJ International Conference on Intelligent Robots and Systems (IROS)*. IEEE, 2020, pp. 2338–2345.
- [5] B. Zhou, P. Krähenbühl, and V. Koltun, "Does computer vision matter for action?" *Science Robotics*, vol. 4, no. 30, p. eaaw6661, 2019.
- [6] A. Prakash, K. Chitta, and A. Geiger, "Multi-modal fusion transformer for end-to-end autonomous driving," in *Proceedings of the IEEE/CVF Conference on Computer Vision and Pattern Recognition*, 2021, pp. 7077–7087.
- [7] I. Sobh, L. Amin, S. Abdelkarim, K. Elmadawy, M. Saeed, O. Abdeltawab, M. Gamal, and A. El Sallab, "End-to-end multi-modal sensors fusion system for urban automated driving," 2018.
- [8] F. Munir, S. Azam, B.-G. Lee, and M. Jeon, "Multi-modal fusion for sensorimotor coordination in steering angle prediction," *arXiv preprint arXiv:2202.05500*, 2022.
- [9] F. Codevilla, M. Müller, A. López, V. Koltun, and A. Dosovitskiy, "End-to-end driving via conditional imitation learning," in *2018 IEEE international conference on robotics and automation (ICRA)*. IEEE, 2018, pp. 4693–4700.
- [10] A. Zhao, T. He, Y. Liang, H. Huang, G. V. d. Broeck, and S. Soatto, "Sam: Squeeze-and-mimic networks for conditional visual driving policy learning," *arXiv preprint arXiv:1912.02973*, 2019.
- [11] Z. Zhang, A. Liniger, D. Dai, F. Yu, and L. Van Gool, "End-to-end urban driving by imitating a reinforcement learning coach," in *Proceedings of the IEEE/CVF International Conference on Computer Vision*, 2021, pp. 15 222–15 232.
- [12] J. Chen, S. E. Li, and M. Tomizuka, "Interpretable end-to-end urban autonomous driving with latent deep reinforcement learning," *IEEE Transactions on Intelligent Transportation Systems*, 2021.
- [13] A. Vaswani, N. Shazeer, N. Parmar, J. Uszkoreit, L. Jones, A. N. Gomez, Ł. Kaiser, and I. Polosukhin, "Attention is all you need," *Advances in neural information processing systems*, vol. 30, 2017.
- [14] A. Dosovitskiy, L. Beyer, A. Kolesnikov, D. Weissenborn, X. Zhai, T. Unterthiner, M. Dehghani, M. Minderer, G. Heigold, S. Gelly *et al.*, "An image is worth 16x16 words: Transformers for image recognition at scale," *arXiv preprint arXiv:2010.11929*, 2020.
- [15] N. Carion, F. Massa, G. Synnaeve, N. Usunier, A. Kirillov, and S. Zagoruyko, "End-to-end object detection with transformers," in *European conference on computer vision*. Springer, 2020, pp. 213–229.
- [16] H. Shao, L. Wang, R. Chen, H. Li, and Y. Liu, "Safety-enhanced autonomous driving using interpretable sensor fusion transformer," *arXiv preprint arXiv:2207.14024*, 2022.
- [17] Z. Huang, X. Mo, and C. Lv, "Multi-modal motion prediction with transformer-based neural network for autonomous driving," in *2022 International Conference on Robotics and Automation (ICRA)*. IEEE, 2022, pp. 2605–2611.
- [18] J. Dong, S. Chen, S. Zong, T. Chen, and S. Labi, "Image transformer for explainable autonomous driving system," in *2021 IEEE International Intelligent Transportation Systems Conference (ITSC)*. IEEE, 2021, pp. 2732–2737.
- [19] L. L. Li, B. Yang, M. Liang, W. Zeng, M. Ren, S. Segal, and R. Urtasun, "End-to-end contextual perception and prediction with interaction transformer," in *2020 IEEE/RSJ International Conference on Intelligent Robots and Systems (IROS)*. IEEE, 2020, pp. 5784–5791.
- [20] F. Codevilla, E. Santana, A. M. López, and A. Gaidon, "Exploring the limitations of behavior cloning for autonomous driving," in *Proceedings of the IEEE/CVF International Conference on Computer Vision*, 2019, pp. 9329–9338.
- [21] D. Chen, B. Zhou, V. Koltun, and P. Krähenbühl, "Learning by cheating," in *Conference on Robot Learning*. PMLR, 2020, pp. 66–75.
- [22] O. Natan and J. Miura, "End-to-end autonomous driving with semantic depth cloud mapping and multi-agent," *IEEE Transactions on Intelligent Vehicles*, 2022.
- [23] M. Liang, B. Yang, W. Zeng, Y. Chen, R. Hu, S. Casas, and R. Urtasun, "Pnpnet: End-to-end perception and prediction with tracking in the loop," in *Proceedings of the IEEE/CVF Conference on Computer Vision and Pattern Recognition*, 2020, pp. 11 553–11 562.
- [24] M. Liang, B. Yang, Y. Chen, R. Hu, and R. Urtasun, "Multi-task multi-sensor fusion for 3d object detection," in *Proceedings of the IEEE/CVF Conference on Computer Vision and Pattern Recognition*, 2019, pp. 7345–7353.

Shoaib Azam received a B.S. degree in Engineering Sciences from Ghulam Ishaq Khan Institute of Science and Technology, Pakistan, in 2010, and an M.S. degree in Robotics and Intelligent Machine Engineering from National University of Science and Technology, Pakistan, in 2015. He received his Ph.D. degree from Gwangju Institute of Science and Technology, Gwangju, South Korea, in 2021. Currently he is working as a postdoctoral researcher, at Gwangju Institute of Science and Technology, South Korea, where he is working on developing end-to-end solutions using deep learning for autonomous driving and robotics. His research interests includes deep learning, autonomous driving, sensorimotor learning, and representation learning.



Farzeen Munir received a B.S. degree in Electrical Engineering from Pakistan Institute of Engineering and Applied Sciences, Pakistan in 2013, and an M.S. degree in System Engineering from Pakistan Institute of Engineering and Applied Sciences, Pakistan in 2015. She received her Ph.D. degree from Gwangju Institute of Science and Technology, Gwangju, South Korea, in 2022. Currently she is working as a postdoctoral researcher, at Gwangju Institute of Science and Technology, South Korea, where she is working

on developing perception and navigation problems related to indoor mobile robotics. Her current research interests include, machine Learning, deep neural network, autonomous driving and computer vision.





Moongu Jeon received a B.S. degree in Architectural Engineering from Korea University, Seoul, South Korea, in 1988, and M.S. and Ph.D. degrees in Computer Science and Scientific Computation from the University of Minnesota, Minneapolis, MN, USA, in 1999 and 2001, respectively. As a Post-Graduate Researcher, he worked on optimal control problems at the University of California at Santa Barbara, Santa Barbara, CA, USA, from 2001 to 2003, and then moved to the National Research Council of Canada, where he worked on the sparse representation of high-dimensional data and image processing until 2005. In 2005, he joined the Gwangju Institute of Science and Technology, Gwangju, South Korea, where he is currently a Full Professor with the School of Electrical Engineering and Computer Science. His current research interests are in machine learning, computer vision, and artificial intelligence.